J. Am. Soc. Mass Spectrom. (2015) 26:1233–1241
DOI: 10.1007/s13361-015-1098-x

RESEARCH ARTICLE

GPU Assisted Simulation Study of Ion–Ion Reactions within Quadrupole Ion Traps

Dan Guo,[1] Muyi He,[1] Yuzhuo Wang,[1] Xingchuang Xiong,[2] Xiang Fang,[2] Wei Xu[1]

[1]School of Life Science, Beijing Institute of Technology, Beijing, 100081, China
[2]National Institute of Metrology, Beijing, 100013, China

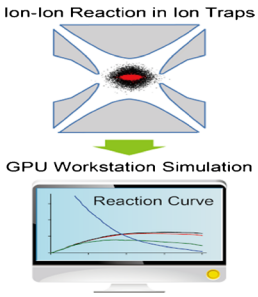

Abstract. In this study, a gas-phase ion–ion reaction model was developed, and it was integrated into an ion trajectory simulation program. GPU parallel computation techniques were also applied to accelerate the simulation process. With this simulation tool, the dependence of ion–ion reaction rate within 3D quadrupole ion traps on both ion trap operation parameters and the characteristics of reaction pair were investigated. It was found that the *m/z* values and charge states of ions have significant influences on the reaction rate. Moreover, higher ion–ion reaction rate was achieved under higher trapping voltages and higher buffer gas pressures. Furthermore, secondary reaction and/or neutralization of ETD fragment ions were observed from simulation. The reaction and/or neutralization rate depends on the charge state and *m/z* of each fragment ion.

Key words: Ion trap, Ion–ion reaction, Electron transfer dissociation, Secondary reaction

Received: 9 October 2014/Revised: 28 November 2014/Accepted: 9 February 2015/Published Online: 14 April 2015

Introduction

Gas-phase ion–ion reaction is an important phenomenon observed in mass spectrometry experiments, in which different types of charge transfers would happen, such as proton transfer, electron transfer, anion attachment, anion transfer, and many others [1]. Due to the advent of electrospray ionization [2], study of ion–ion reaction is not restricted to singly charged ions, but also involves multiply charged ions. The dissociation reactions of multiply charged biomolecules, such as ETD (electron transfer dissociation) [3, 4] and NETD (negative ETD) [5, 6], have been widely applied in the structure analyses of biomolecules, especially for proteins with post-translational modifications [7–10].

Ion–ion reactions, especially ETD, have been realized and implemented in ion trap mass spectrometers and hybrid instruments. The first instrument used for ion–ion reaction study was a Y-tube/quadrupole mass filter in which ions reacted under near atmospheric pressure region and charge reduction was observed [11]. After that, a lot of ion–ion reaction experiments were performed in vacuum to have a better control of the reaction condition [12–15]. Different from ion–electron interactions, which are normally performed in Fourier transform ion cyclotron resonance cells (FT-ICR) [16, 17], ion–ion reactions are typically carried out in quadrupole ion traps and multi-pole cells [18–21]. With the capability of trapping cations and anions at the same time, both 3D and linear ion traps have been modified to realize ETD functions [22, 23].

Ion–ion reaction rate is a very important factor in the application of ETD or other types of ion–ion reactions. The dependence of proton transfer reaction rate on charge state and types of reactant was explored through experiments [13]. To manipulate ion–ion reaction, a method called "ion parking" can inhibit the reaction rate of a specific ion, in which an AC potential was applied on the endcap of a 3D quadrupole ion trap to reduce the spatial overlap and increase the relative velocity of ions [24–26]. Furthermore, the use of DC potential to control ion–ion reaction rate in ion traps was also reported [27, 28]. Although ETD has the advantage of providing complementary structure information to collision induced dissociation (CID) [29–31], ETD still suffers from relatively low product ion intensity and slow reaction rate [32]. To address these issues, experiments were also performed to accelerate the reaction process by optimizing ion trap operation parameters and the selection of reactant partners [32]. Considerable theoretical efforts have also been devoted to study ion–ion reaction

Electronic supplementary material The online version of this article (doi:10.1007/s13361-015-1098-x) contains supplementary material, which is available to authorized users.

Correspondence to: Wei Xu; *e-mail:* weixu@bit.edu.cn

kinetics [13]; however, there is a still lack of a theoretical model and simulation tools to provide us with a deeper understanding of the reaction process.

In this study, a new ion–ion reaction model was developed, which could be used to calculate ion–ion reaction cross sections and to model the formation of Coulombically bond orbital complexes of ions. Then, the theoretical model was integrated into the ion trajectory simulation program developed in our lab earlier [27, 33, 34]. Since the simulation of ion–ion interaction is a time-consuming process, GPU parallel computation techniques were applied to accelerate the simulation process. With the simulation tool developed in this work, the dependence of ion–ion reaction rate on ion trap operation parameters and the characteristics of reaction pair were investigated. Operation parameters, such as buffer gas pressure, ion trapping q value, m/z values of cations and anions, were optimized for maximized ion–ion reaction rate. With the assumption that a charge transfer could initiate an ETD reaction, the product ion loss phenomenon (or secondary ion reaction) was found in ETD experiments. Simulation results show that as high as ~74% of product ions (cations) could further react with anions in extreme cases, which results in decreased product ion intensities.

Ion–Ion Reaction Modeling

To be able to simulate the ion–ion reaction process, a suitable theoretical ion–ion reaction model is required, which predicts the ion–ion reaction probability (or ion reaction cross section, RCS); in other words, under what circumstance an ion will react with another ion (ion velocity and relative position). This theoretical model could then be implemented in an ion trajectory simulation program, and the ion–ion reaction process could be simulated afterwards.

Theoretical Modeling

Although many collision models exist for ion–molecule collisions, such as the Langevin collision model, the hard-sphere collision model, and the mixed collision model [35], no ion–ion reaction model has been proposed and implemented in ion trajectory simulations. Estimated reaction rates could be found in literature [13], however, without detailed derivations. In this work, a practical ion cloud distribution, Gaussian distributions, was considered, instead of uniform ion distributions typically assumed in previous works [14]. For the first time, an effective potential curve and ion–ion reaction model were derived specifically for ion–ion reactions in this study.

Different from ion–molecule interactions, the Coulomb force between two ions with different polarities would be the dominant force in the ion–ion interactions. Nevertheless, there are similarities between the Langevin collision model and the ion–ion reaction model. In the Langevin collision model, the ion–neutral interaction is modeled as the Coulomb force between a point charge and the charge induced dipole within the neutral molecule, which would be weaker than that between two ions [36–38]. Following the Langevin collision model, an ion–ion reaction would happen when the ion can overcome the centrifugal barrier between these two ions and be "trapped" by another.

When two ions are close to each other before reaction happens, Coulomb force is assumed to be the dominant force, and according to the law of conservation of energy:

$$E_0 = E_{\mathrm{rel0}} - \frac{kq_1q_2}{r_0} = \frac{1}{2}\mu r'^2 + E_{\mathrm{rel0}}\left(\frac{b}{r}\right)^2 - \frac{kq_1q_2}{r} \tag{1}$$

in which E_0 is the total energy of this system, E_{rel0} is the initial relative kinetic energy, r_0 is the initial distance between two ions, k is the Coulomb constant, q_1 and q_2 are the charges two ions possess, respectively, μ is the relative mass, r is the distance between two ions, b is the impact parameter, which is the minimum distance these two ions approach in the absence of attraction force between them (detailed definition of b can be found in reference [38].

The right side of Equation 1 can be treated as the summation of a translational energy term and a distance dependentent term, which could be defined as the effective potential.

$$V_{\mathrm{eff}} = E_{\mathrm{rel0}}\left(\frac{b}{r}\right)^2 - \frac{kq_1q_2}{r} \tag{2}$$

Therefore, the total energy is the summation of the translational energy and the effective potential.

Because the attractive force between two ions is different from that between an ion and a molecule, the interactions between two ions have quite different features. Figure 1a shows a typical effective potential curve, which decreases first and then increases rapidly as two ions approaching each other. As $\frac{1}{2}\mu r'^2 \geq 0$, according to Equation 1, $V_{\mathrm{eff}} \leq E_0$. At the nearest point or the apogee point of the orbit, the relative velocity vector is perpendicular to the position vector, the translation energy equals zero and the effective potential equals the total energy. If the total energy of the system $E_0 \geq 0$, there will be only one intersection point (point A or B in Figure 1a) between the effective potential curve and line $E=E_0$. In this situation, the relative trajectory of these two ions is divergent, so these two ions will "pass by" each other. If the total energy of the system $E_0<0$, the effective potential curve has two intersection points (point C and D in Figure 1a) with line $E=E_0$, so the relative trajectory (or orbit) of these two ions is a closed curve, in other words, one ion is "trapped" by the other ion. When a stable orbit is formed between these two ions, both electron transfer and proton transfer could happen in this reaction process, which highly depends on the chemical natures of these two ions. For simplicity, the rate of forming Coulombically bond orbital complexes is used to estimate the ion–ion reaction rate in this work.

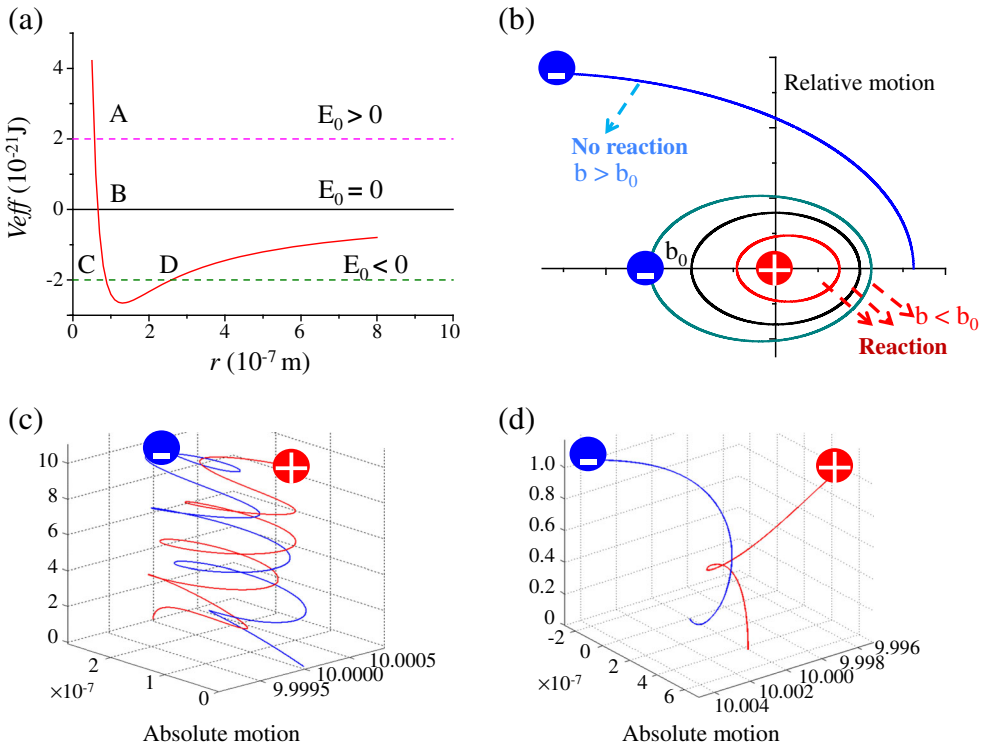

Figure 1. (**a**) The effective potential versus the distance between two ions curve. (**b**) The relative motion between two ions under different initial conditions. (**c**), (**d**) The absolute trajectories of two ions within a 3D ion trap under initial condition of $b<b_0$ (**c**) and $b>b_0$ (**d**)

For the reaction cross section, the critical condition that two ions will form a stable orbit would be

$$b_0 = \frac{kq_1q_2}{E_{\text{rel0}}} \tag{3}$$

which was obtained by setting E_0=0 in Equation 1. The reaction constant can then be written as:

$$k_c = v\, n\, \pi \left(\frac{k\, q_1 q_2}{E_{\text{rel0}}}\right)^2 \tag{4}$$

in which v is the average velocity of ions and n is the density of reactant partners. Figure 1b plots some typical ion relative trajectories when b is less than b_0 (circular or elliptical orbit) and larger than b_0 (open curve, which is a parabolic curve when b equals b_0). Simulated ion trajectories in the absolution Cartesian coordinate are shown in Figure 1c (ion–ion reaction, $b<b_0$) and 1d (ion–ion passing by, $b>b_0$).

It can be seen from Equation 4 that the ion–ion reaction rate is in proportion to ion number density and the square of ion charges. The ion number density and the relative spatial distribution of anions and cations are affected by the mass-to-charge ratios of ions and ion trap operation parameters. Detailed derivation of the relationship between reaction constant and ion trap operation parameters can be found in the Supplementary Information.

Numerical Implementation

In this study, reactions of multiply charged cations and singly charged anions in ideal 3D ion traps with pure quadrupole electric fields and dimensions of r_0=5 mm and z_0=3.536 mm (center to electrodes) were investigated. The ion trajectory simulation program developed in our lab was used [34]. The ion motion differential equation, which takes Coulomb forces into consideration, was solved using the fourth Runge-Kutta integration method. Helium was used as the buffer gas and the hard-sphere collision model was applied to model the ion–neutral collisions. Since the cations studied in this work have high masses, the hard-sphere collision model is more realistic than the Langevin collision model [35]. The calculation of energy transfer of ion and neutral molecules is based on the assumption of elastic collision. The simulation step is 10 ns to minimize numerical integration error. At the beginning of the simulation, ions are placed in the center of the ion trap, and the velocities of ions are in Gaussian distribution with a given standard deviation. After the size of ion cloud becomes stable, the simulation of ion–ion reaction begins to run.

Ion–ion reaction model was integrated in the ion trajectory simulation program as follows: for each ion, pick up the nearest oppositely charged ion at every time step; if the distance is smaller than the given value ($2*10^{-7}$ m), judge whether they could form an orbital complex by the total energy; if two ions could form an orbital complex, reaction happens and anion transfers an electron to cation; as a result, the anion becomes a neutral and the charges of cation minus one (details in Supplementary Information).

In this simulation, both the calculations of Coulomb forces and ion–ion reactions are time-consuming processes. Multi-core CPU in a single computer can hardly be burdened with such a large amount of calculation. To accelerate the simulation

process, a GPU card (NVIDIA tesla k40c with 2880 compute unified device architecture (CUDA) cores) was used to run these two parts of simulations. Details about integrating GPU technique in ion trajectory simulation can be found in our earlier work [34].

Results and Discussions

In ETD experiments, it is important to optimize instrument operation parameters to maximize fragment ion intensity, which is highly related with ion–ion reaction rates. Different ions and operation conditions have significant impacts on reaction rates, so it is critical to know the influence of different parameters on ion–ion reactions. Generally speaking, ion–ion reaction rate is highly related with factors, which would affect ion cloud distribution and the Coulomb interaction force between ions. In this study, the simulation conditions were set as follows (otherwise specified): 30,000 anions (azobenzene, 182.2 Da) and 10,000 cations (angiotensin I, 1299 Da) were placed in the 3D ion trap, with helium as the buffer gas and pressure 1 mTorr; rf signal: 1 MHz, 300 $V_{0\text{-p}}$.

m/z Values of Cations

In typical ETD experiments, cations are multiply protonated proteins or polypeptides and anions are electron donors with relatively low m/z. Typically, the m/z values of cations are larger than those of anions. It is found from simulation (Figure 2a) that the larger the cation is (with fixed anion, azobenzene, 182.2 Da; fixed ion trap operation condition, rf voltage $V_{0\text{-p}}$= 300 V), the lower the reaction rate would be. Under the same trapping voltage, the difference in *m/z* between cations and anions would lead to different ion cloud distributions [34, 39], which reduce the spatial overlap of cations and anions (see Figure 2b and c). Mathematically, further overlapping of these two ion clouds would increase the ion number density (n) in Equation 4, and thus the increase of ion reaction rate. The reaction rate versus cation *m/z* follows the form of $\frac{A}{1+B\left(\frac{m}{z}\right)}$, in which A and B are fitting parameters.

Charge States of Cations

It has been found from experimental results that the reaction rates of ETD reactions highly depend on the charge state of the cations [9]. Typically, the higher the charge state the easier an ETD reaction would happen, as well as the fragmentation efficiency. However, it is not easy to separate the charge state effects from other effects in experiments, since the change of charge states would normally also change the trapping q_z and the *m/z* difference between cations and anions. On the other hand, simulation is a very convenient tool to isolate the effect of charge state. Figure 3a shows the dependence of ion reaction rate with respect to cation charge state, while keeping all other parameters constant (cation 182.2 Da, anion *m/z* 433 Da, q_z 0.64 for anion, helium pressure 1 mTorr). As a result, a close to linear relationship was obtained. The more charges cations possess, the stronger the force between cations and anions will be. Yet at the same time, the repulsive force between cations also increases, which leads to a bigger cation cloud, and thus smaller ion density (Figure 3b). Therefore, the increase of reaction rate is a counterbalance between stronger cation–anion attraction forces and thinner cation densities (Equation 4). Since the anion cloud size or density has very small variation along with the increase of cation charge state, the reaction rate with respect to cation charge state has a close to linear relationship $\left(\frac{A\,z^2}{B+z}\right)$ mathematically. Detailed discussions can be found in the Supplementary Information. In ion–ion proton transfer reaction experiments, charge states and *m/z* values have been changed at the same time, and the reaction rate is found to be in proportion to the square of ion charge [13].

Ion Number

Ion number will have effects on ion cloud size and density [34, 39], when other parameters are kept the same. Simulation results in Figure 4a show that ion–ion reaction rate increases with the increase of anion number until it reaches a plateau, which agrees with the results from experiments [32]. In the simulation, while increasing the number of anions, the number of cations was kept at 10^4. With more anions, a cation will experience stronger Coulomb attraction forces from anions, which results in a tighter cation cloud as shown in Figure 4b, and thus faster ion–ion reaction rate. This ion–ion attraction phenomenon has been found in earlier experiments, in which the trapping of high *m/z* ions can be improved when a large population of oppositely charged low *m/z* ions exists in the same trap [40]. A similar phenomenon was also observed through simulation (Figure S2 in the Supporting Information). When the number of anion is much larger than that of cation, the increase of anion number will have little effect on ion–ion reaction rates.

Ion Trapping Voltage

During an ion–ion reaction process in a quadrupole ion trap, the trapping voltage will change the ion distributions [34, 39, 41–43], and therefore the reaction rates as shown in Figure 5a. A deeper pseudo-potential trapping well formed at higher q values (q<0.7) results in tighter ion clouds (Figure 5b). Although ions would have higher kinetic energy at higher trapping voltages, which may reduce the reaction cross section, the ion–ion reaction rate still increases as trapping electric voltage increases. In a practical ion–ion reaction experiment, ion reaction rate could be increased by applying higher trapping voltage, which was also confirmed in experiments [32]. However, a relatively acceptable low-mass cutoff needs

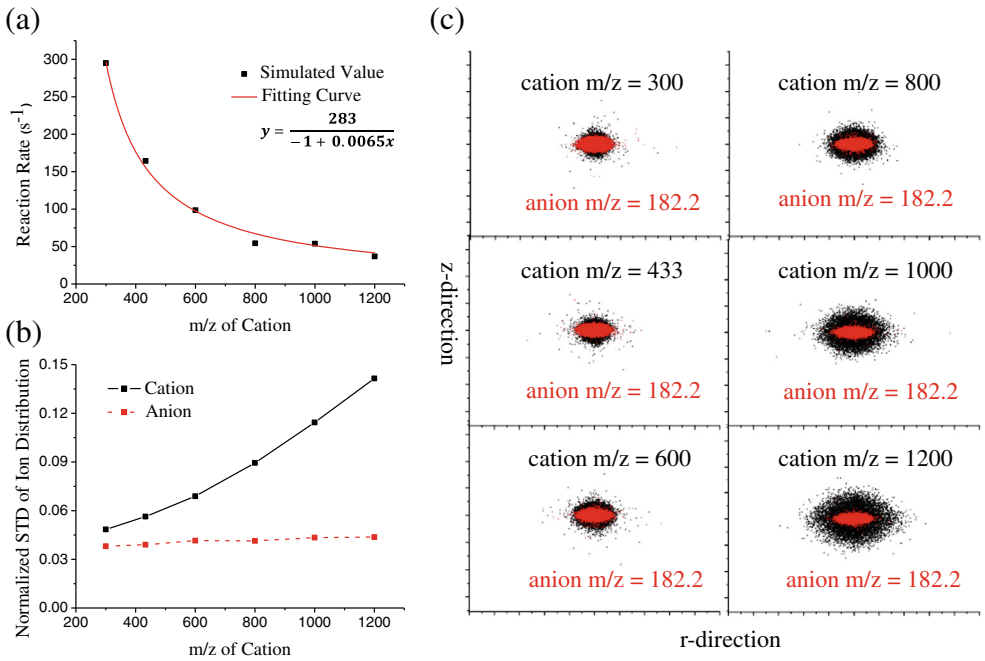

Figure 2. The reaction rate versus m/z value of cation curve (**a**) and the corresponding ion cloud size (**b**), ion distribution (**c**). Cation: z=3, ion number=10^4, anion: m/z=182.2, z=–1, ion number=3*10^4, trapping voltage 300 V, helium pressure 5 mTorr

to be maintained so that small product ions could still be observed.

Buffer Gas Pressures

Buffer gas could remove the excrescent kinetic energy of ions and cool ions to the center of ion traps. With condensed ion distributions, the ion reaction rate could be increased by increasing the buffer gas pressure (Figure 6a). As shown in Figure 6b, the size of the cation cloud would decrease as the buffer gas pressure increases, and it reaches a plateau when the pressure reaches to ~7 mTorr, which agrees well with previous simulation and experimental results [44–46]. In conventional ion trap mass spectrometers, the increase of buffer gas pressure would cause degraded mass resolution. Buffer gas pressure could be increased to speed up the ion–ion reactions in modern mass spectrometers, especially for hybrid instruments, where the ion reaction and mass analyses are performed in separated devices.

Secondary Reactions in ETD Experiments

In an ETD experiment, fragmentation pattern and the abundance of product ions are important parameters in MASCOT database searching [47], which directly affects the accuracy of protein or peptide identification. Different from a CID experiment, the product ions in an ETD reaction could undergo further reactions with anions (assuming precursor ions have positive charges). This further reaction would neutralize singly charged product ions, which will lower the product ion abundance. Furthermore, product ions with different m/z values and

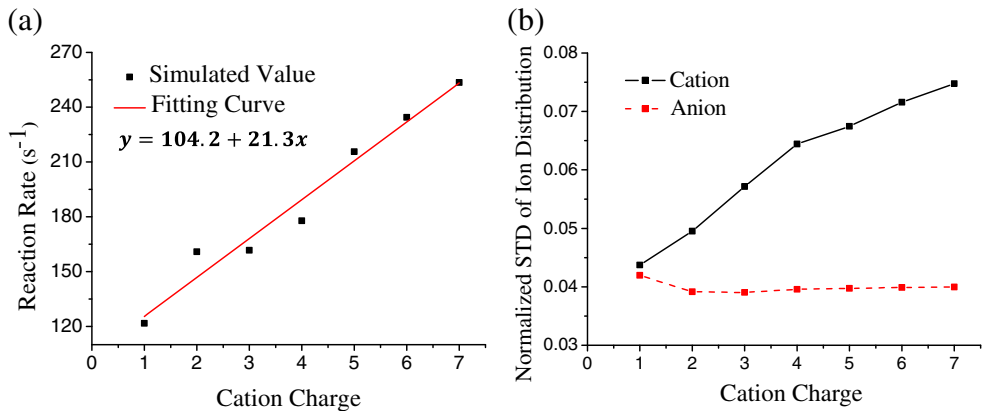

Figure 3. The reaction rate versus number of charges on cation (**a**) and the corresponding ion cloud size (**b**). Cation: m/z=433, ion number=10^4, anion: m/z=182.2, z=–1, ion number=3*10^4, trapping voltage 300 V, helium pressure 5 mTorr

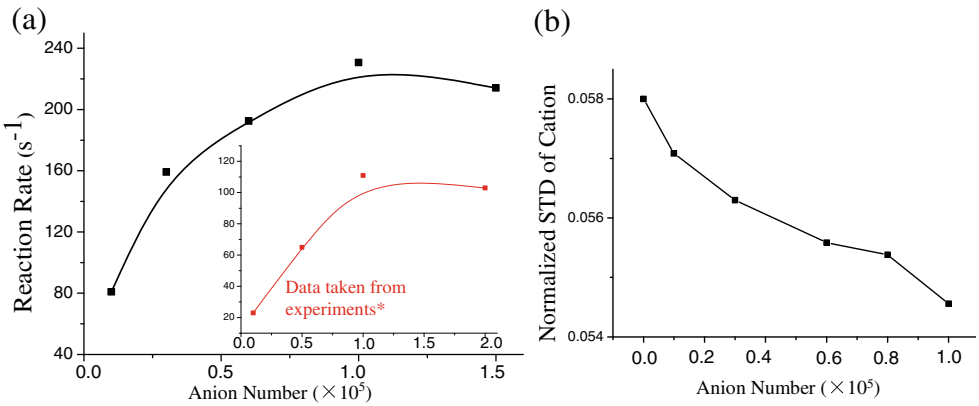

Figure 4. (**a**) The reaction rate versus anion number; inset: reaction rate taken from experimental results in literature. (**b**) The corresponding ion cloud size. Cation: m/z=433, z=3, ion number=10^4, anion: m/z=182.2, z=–1, trapping voltage 300 V, helium pressure 5 mTorr. *Data was evaluated from Compton et al., 2012 [32]

charges have different reaction rates, which will then change the tandem mass spectrum pattern. In this simulation study, the ETD reaction of angiotensin I with +3 charges was investigated under optimized conditions: rf trapping voltage 300 $V_{0\text{-}p}$, buffer gas pressure 7 mTorr. To simplify the simulation process, the following assumptions have been made: only three representative product ions of angiotensin I (c_3, z_8, and c_9^{++}) were considered, and there is an equal probability of generating each type of fragment ions when an ion–ion reaction happens between angiotensin I with azobenzene. The abundances of angiotensin I ions and product ions at different times are shown in Figure 7a. The dashed curves represent the generated product ions, and the solid curves represent the remaining product ions after secondary reactions with anions. The simulated tandem mass spectrum of angiotensin I with 3, 5, and 8 ms reaction times was plotted in Figure 7b, c, and d, respectively. Product ions with multiple charges (c_9^{++}) would have a much larger chance of undergoing secondary reactions with anions, as well as for the product ions whose m/z are close to that of the anions (c_3). Furthermore, at the beginning of ETD reactions, product ion intensities increase with increased reaction durations. However, product ion intensities do not always increase, but actually decrease with longer reaction durations because of secondary ion reactions. Similar results have also been found in experiments [32].

Simulation Versus Experiment

Results from simulations were compared with those from experiments. In general, many phenomena in experiments could be well observed in simulations (as discussed earlier), and actual reaction rates are on the same order. For instance, the simulated reaction rate of angiotensin I (3+) was about 41 s^{-1} (1 mTorr, cation 10^4, anion $3*10^4$), as shown in Figure 6a. In experiments, very similar a reaction rate (45 s^{-1}) was found for vasoactive intestinal peptide (1−12, m/z 475 Da, z=3+) at similar working conditions. However, there are very limited data that could be compared with experiments, since the experiment results available were obtained in a commercial linear ion trap at 1 mTorr [32]. Most of the results in this work were obtained in an ideal 3D ion trap at 5 or 7 mTorr. Since higher

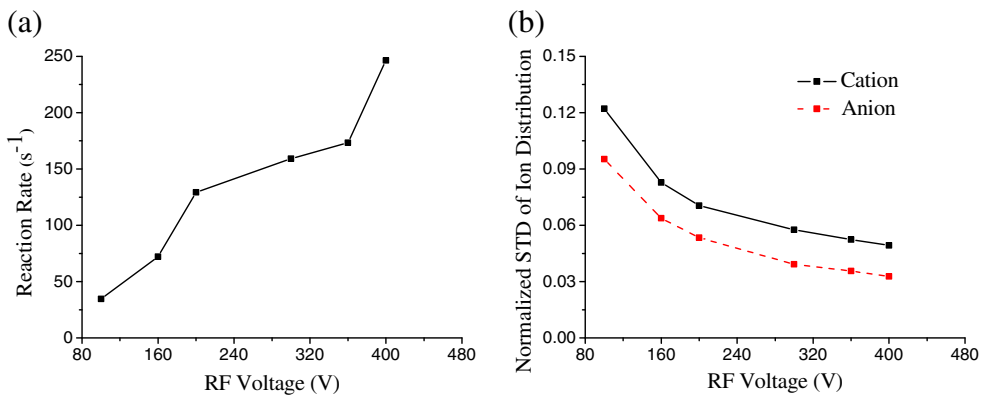

Figure 5. The reaction rate versus rf voltage curve (**a**) and the corresponding ion cloud size (**b**). Cation: m/z=433, z=3, ion number=10^4, anion: m/z=182.2, z=–1, ion number=$3*10^4$, helium pressure 5 mTorr

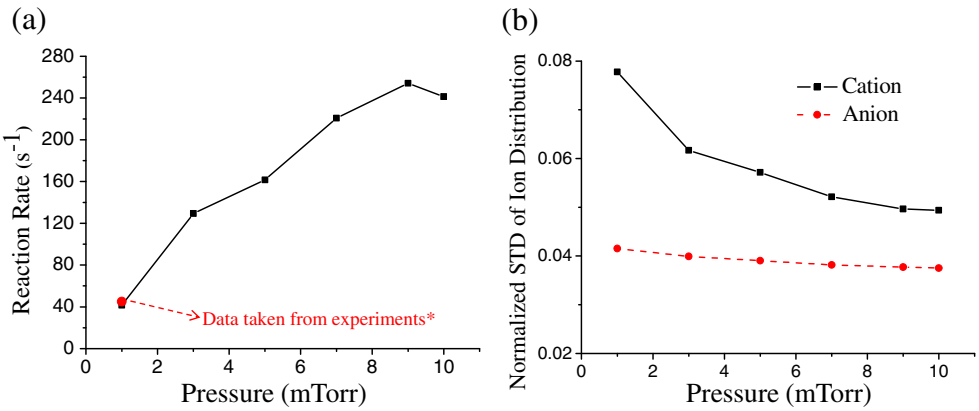

Figure 6. The reaction rate versus pressure curve (**a**) and the corresponding ion cloud size (**b**). Cation: m/z=433, z=3, ion number=10^4, anion: m/z=182.2, z=–1, ion number=3*10^4, trapping voltage 300 V. *Data was evaluated from Compton et al., 2012 [32]

pressure would improve the ion reaction speed (Figure 6a), this optimized pressure condition was used in simulations (an ion trap and most electron multipliers will not work well at higher pressures practically [45, 48]). The ion reaction rate would be ~4 times higher at 5 mTorr than that at 1 mTorr for the presence of 10^4 cation and 3*10^4 anions as shown in Figure 6a. In fact,

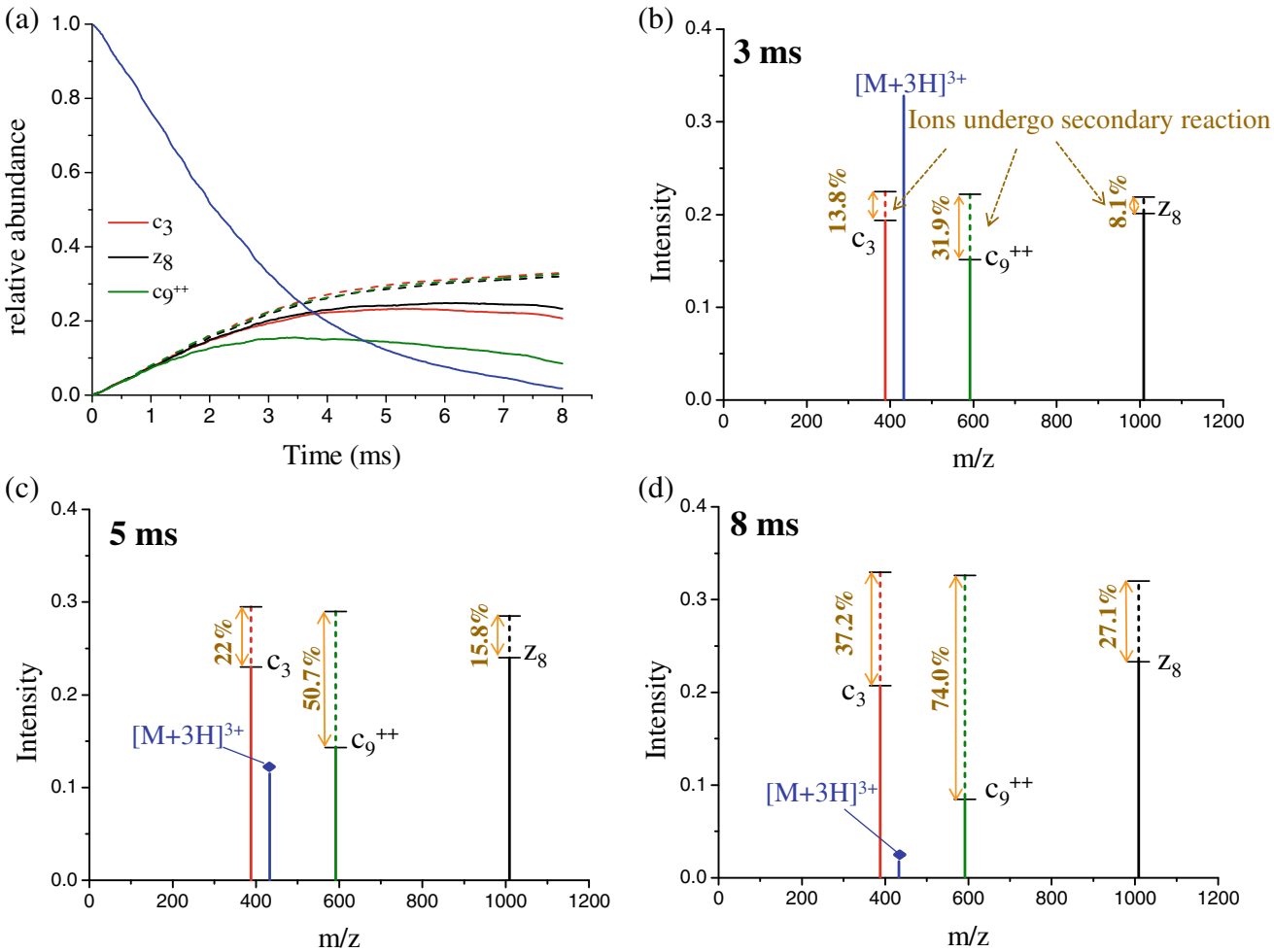

Figure 7. The neutralization of ETD fragments of angiotensin I (3+). (**a**) The abundance of precursor ions and fragment ions along with time. The dashed lines represent fragment ions that were generated by precursor ions and the solid lines represent fragment ions remained in the ion trap. The corresponding mass spectra (**b**) at 3 ms; (**c**) at 5 ms, and (**d**) at 8 ms. Cation: m/z=433, z=3, ion number=10^4, anion: m/z=182.2, z=–1, ion number=3*10^4, trapping voltage 300 V, helium pressure, 7 mTorr

the simulated ion reaction rate of angiotensin I (3+) at 5 mTorr (Figure 4a, cation 10^4, anion 1–5*10^4) is about three to four times of the measured ion reaction rates at 1 mTorr (Figure 4a inset extracted from reference [32], cation 10^4, anion 1–5*10^4).

The ETD reaction time in Figure 7 is much shorter than in conventional experiments, which is because simulation was performed at 7 mTorr. The ion reaction rate at 7 mTorr was about five to six times larger than that at 1 mTorr (Figure 6a). Therefore, the reaction duration in simulation would be five to six times shorter than that in conventional experiments, which are typically performed at 1 mTorr. For instance, maximized fragment ion intensities were obtained at ~5 ms at 7 mTorr in simulation, which is expected to be 25–30 ms in experiments at 1 mTorr. Actually, a 15–20 ms optimized reaction duration was found by monitoring product ion intensities in experiments [32].

Conclusion

A theoretical model and a simulation program accelerated by GPU parallel computing techniques were developed to study ion–ion reactions in quadrupole ion traps for the first time. It was found that the ion–ion reaction rate is related to the ion cloud density and ion charge states. A higher reaction rate can be achieved under higher trapping voltages (q<0.87), higher pressures, higher charge states, and for a reaction pair with closer *m/z* values. Simulation shows that ETD product ions would undergo further reactions and/or neutralizations, which cause the decrease of product ion intensities. The ratio of product ion loss depends on their *m/z* and number of charges, and as high as 74% of the product ions could be lost in specific conditions. Theoretical and simulation results could be applied as a guideline for the optimization of ETD reactions.

Acknowledgments

The authors acknowledge support for his work by MOST China (2011YQ0900502 and 2012YQ040140-07), NNSF of China (21205005 and 21475010), and 1000 Plan China.

References

1. McLuckey, S.A., Stephenson, J.L.: Ion/ion chemistry of high-mass multiply charged ions. Mass Spectrom. Rev. **17**(6), 369–407 (1998)
2. Fenn, J.B., Mann, M., Meng, C.K., Wong, S.F., Whitehouse, C.M.: Electrospray ionization for mass spectrometry of large biomolecules. Science **246**(4926), 64–71 (1989)
3. Syka, J.E.P., Coon, J.J., Schroeder, M.J., Shabanowitz, J., Hunt, D.F.: Peptide and protein sequence analysis by electron transfer dissociation mass spectrometry. Proc. Natl. Acad. Sci. U. S. A. **101**(26), 9528–9533 (2004)
4. Vincent, C.E., Rensvold, J.W., Westphall, M.S., Pagliarini, D.J., Coon, J.J.: Automated gas-phase purification for accurate, multiplexed quantification on a stand-alone ion-trap mass spectrometer. Anal. Chem. **85**(4), 2079–2086 (2013)
5. Coon, J.J., Shabanowitz, J., Hunt, D.F., Syka, J.E.P.: Electron transfer dissociation of peptide anions. J. Am. Soc. Mass Spectrom. **16**(6), 880–882 (2005)
6. Huzarska, M., Ugalde, I., Kaplan, D.A., Hartmer, R., Easterling, M.L., Polfer, N.C.: Negative electron transfer dissociation of deprotonated phosphopeptide anions: choice of radical cation reagent and competition between electron and proton transfer. Anal. Chem. **82**(7), 2873–2878 (2010)
7. Udeshi, N.D., Compton, P.D., Shabanowitz, J., Hunt, D.F., Rose, K.L.: Methods for analyzing peptides and proteins on a chromatographic timescale by electron-transfer dissociation mass spectrometry. Nat. Protoc. **3**(11), 1709–1717 (2008)
8. Hart-Smith, G.: A review of electron-capture and electron-transfer dissociation tandem mass spectrometry in polymer chemistry. Anal. Chim. Acta **808**, 44–55 (2014)
9. Wiesner, J., Premsler, T., Sickmann, A.: Application of electron transfer dissociation (ETD) for the analysis of posttranslational modifications. Proteomics **8**(21), 4466–4483 (2008)
10. Myers, S.A., Daou, S., Affar, E.B., Burlingame, A.: Electron transfer dissociation (ETD): the mass spectrometric breakthrough essential for O-GlcNAc protein site assignments—a study of the O-GlcNAcylated protein host cell factor C1. Proteomics **13**(6), 982–991 (2013)
11. Ogorzalek Loo, R.R., Udseth, H.R., Smith, R.D.: A new approach for the study of gas-phase ion-ion reactions using electrospray ionization. J. Am. Soc. Mass Spectrom. **3**(7), 695–705 (1992)
12. Herron, W.J., Goeringer, D.E., McLuckey, S.A.: Ion–ion reactions in the gas phase: proton transfer reactions of protonated pyridine with multiply charged oligonucleotide anions. J. Am. Soc. Mass Spectrom. **6**(6), 529–532 (1995)
13. Stephenson, J.L., McLuckey, S.A.: Ion/ion reactions in the gas phase: proton transfer reactions involving multiply-charged proteins. J. Am. Chem. Soc. **118**(31), 7390–7397 (1996)
14. Stephenson, J.L., Van Berkel, G.J., McLuckey, S.A.: Ion–ion proton transfer reactions of bio-ions involving noncovalent interactions: holomyoglobin. J. Am. Soc. Mass Spectrom. **8**(6), 637–644 (1997)
15. Stephenson, J.L., McLuckey, S.A.: Charge manipulation for improved mass determination of high-mass species and mixture components by electrospray mass spectrometry. J. Mass Spectrom. **33**(7), 664–672 (1998)
16. Zubarev, R.A., Kelleher, N.L., McLafferty, F.W.: Electron capture dissociation of multiply charged protein cations. A nonergodic process. J. Am. Chem. Soc. **120**(13), 3265–3266 (1998)
17. Zubarev, R.A., Horn, D.M., Fridriksson, E.K., Kelleher, N.L., Kruger, N.A., Lewis, M.A., Carpenter, B.K., McLafferty, F.W.: Electron capture dissociation for structural characterization of multiply charged protein cations. Anal. Chem. **72**(3), 563–573 (2000)
18. Reid, G.E., Mitchell Wells, J., Badman, E.R., McLuckey, S.A.: Performance of a quadrupole ion trap mass spectrometer adapted for ion/ion reaction studies. Int. J. Mass Spectrom. **222**(1), 243–258 (2003)
19. Wu, J., Hager, J.W., Xia, Y., Londry, F.A., McLuckey, S.A.: Positive ion transmission mode ion/ion reactions in a hybrid linear ion trap. Anal. Chem. **76**(17), 5006–5015 (2004)
20. Xia, Y., Chrisman, P.A., Erickson, D.E., Liu, J., Liang, X., Londry, F.A., Yang, M.J., McLuckey, S.A.: Implementation of ion/ion reactions in a quadrupole/time-of-flight tandem mass spectrometer. Anal. Chem. **78**(12), 4146–4154 (2006)
21. Xia, Y., McLuckey, S.A.: Evolution of instrumentation for the study of gas-phase ion/ion chemistry via mass spectrometry. J. Am. Soc. Mass Spectrom. **19**(2), 173–189 (2008)
22. Pitteri, S.J., Chrisman, P.A., Hogan, J.M., McLuckey, S.A.: Electron transfer ion/ion reactions in a three-dimensional quadrupole ion trap: reactions of doubly and triply protonated peptides with SO2 center dot. Anal. Chem. **77**(6), 1831–1839 (2005)
23. Liang, X., Hager, J.W., McLuckey, S.A.: Transmission mode ion/ion electron-transfer dissociation in a linear ion trap. Anal. Chem. **79**(9), 3363–3370 (2007)
24. McLuckey, S.A., Reid, G.E., Wells, J.M.: Ion parking during ion/ion reactions in electrodynamic ion traps. Anal. Chem. **74**(2), 336–346 (2002)
25. Chrisman, P.A., Pitteri, S.J., McLuckey, S.A.: Parallel ion parking: improving conversion of parents to first-generation products in electron transfer dissociation. Anal. Chem. **77**(10), 3411–3414 (2005)
26. Chrisman, P.A., Pitteri, S.J., McLuckey, S.A.: Parallel ion parking of protein mixtures. Anal. Chem. **78**(1), 310–316 (2006)
27. Prentice, B.M., Xu, W., Ouyang, Z., McLuckey, S.A.: DC potentials applied to an end-cap electrode of a 3D ion trap for enhanced MSn functionality. Int. J. Mass Spectrom. **306**(2/3), 114–122 (2011)
28. Grosshans, P.B., Ostrander, C.M., Walla, C.A.: Methods and apparatus to control charge neutralization reactions in ion traps. USA Patents US20030155502A1, 2003

29. Sarbu, M., Ghiulai, R., Zamfir, A.: Recent developments and applications of electron transfer dissociation mass spectrometry in proteomics. Amino Acids **46**(7), 1625–1634 (2014)
30. McLuckey, S.A., Mentinova, M.: Ion/neutral, ion/electron, ion/photon, and ion/ion interactions in tandem mass spectrometry: do we need them all? Are they enough? J. Am. Soc. Mass Spectrom. **22**(1), 3–12 (2011)
31. Kim, M.-S., Pandey, A.: Electron transfer dissociation mass spectrometry in proteomics. Proteomics **12**(4/5), 530–542 (2012)
32. Compton, P.D., Strukl, J.V., Bai, D.L., Shabanowitz, J., Hunt, D.F.: Optimization of electron transfer dissociation via informed selection of reagents and operating parameters. Anal. Chem. **84**(3), 1781–1785 (2012)
33. Xu, W., Chappell, W.J., Ouyang, Z.: Modeling of ion transient response to dipolar AC excitation in a quadrupole ion trap. Int. J. Mass Spectrom. **308**(1), 49–55 (2011)
34. Xiong, X.C., Xu, W., Fang, X., Deng, Y.L., Ouyang, Z.: Accelerated simulation study of space charge effects in quadrupole ion traps using GPU techniques. J. Am. Soc. Mass Spectrom. **23**(10), 1799–1807 (2012)
35. He, M., Guo, D., Feng, Y., Xiong, X., Zhang, H., Fang, X., Xu, W.: Realistic modeling of ion-neutral collisions in quadrupole ion traps. J. Mass Spectrom. **50**(1), 95–102 (2015)
36. Langevin, P.: A fundamental formula of kinetic theory. Ann. Chim. Phys. **5**, 245–288 (1905)
37. Su, T., Bowers, M.T.: Ion-folar molecule collisions: the effect of ion size on ion-polar molecule rate constants; the parameterization of the average-dipole-orientation theory. Int. J. Mass Spectrom. Ion Phys. **12**(4), 347–356 (1973)
38. Fernandez-Ramos, A., Miller, J.A., Klippenstein, S.J., Truhlar, D.G.: Modeling the kinetics of bimolecular reactions. Chem. Rev. **106**(11), 4518–4584 (2006)
39. Guo, D., Wang, Y., Xiong, X., Zhang, H., Zhang, X., Yuan, T., Fang, X., Xu, W.: Space charge induced nonlinear effects in quadrupole ion traps. J. Am. Soc. Mass Spectrom. **25**(3), 498–508 (2014)
40. McLuckey, S.A., Wu, J., Bundy, J.L., Stephenson, J.L., Hurst, G.B.: Oligonucleotide mixture, analysis via electrospray and ion/ion reactions in a quadrupole ion trap. Anal. Chem. **74**(5), 976–984 (2002)
41. Hemberger, P.H., Nogar, N.S., Williams, J.D., Cooks, R.G., Syka, J.E.P.: Laser photodissociation probe for ion tomography studies in a quadrupole ion-trap mass spectrometer. Chem. Phys. Lett. **191**(5), 405–410 (1992)
42. Cleven, C.D., Cooks, R.G., Garrett, A.W., Nogar, N.S., Hemberger, P.H.: Radial distributions and ejection times of molecular ions in an ion trap mass spectrometer: a laser tomography study of effects of ion density and molecular type. J. Phys. Chem. **100**(1), 40–46 (1996)
43. Tolmachev, A.V., Udseth, H.R., Smith, R.D.: Radial stratification of ions as a function of mass to charge ratio in collisional cooling radio frequency multipoles used as ion guides or ion traps. Rapid Commun. Mass Spectrom. **14**(20), 1907–1913 (2000)
44. Pekar Second, T., Blethrow, J.D., Schwartz, J.C., Merrihew, G.E., MacCoss, M.J., Swaney, D.L., Russell, J.D., Coon, J.J., Zabrouskov, V.: Dual-pressure linear ion trap mass spectrometer improving the analysis of complex protein mixtures. Anal. Chem. **81**(18), 7757–7765 (2009)
45. Xu, W., Song, Q., Smith, S.A., Chappell, W.J., Ouyang, Z.: Ion trap mass analysis at high pressure: a theoretical view. J. Am. Soc. Mass Spectrom. **20**(11), 2144–2153 (2009)
46. Song, Q., Xu, W., Smith, S.A., Gao, L., Chappell, W.J., Cooks, R.G., Ouyang, Z.: Ion trap mass analysis at high pressure: an experimental characterization. J. Mass Spectrom. **45**(1), 26–34 (2009)
47. Perkins, D.N., Pappin, D.J.C., Creasy, D.M., Cottrell, J.S.: Probability-based protein identification by searching sequence databases using mass spectrometry data. Electrophoresis **20**(18), 3551–3567 (1999)
48. Xu, W., Maas, J., Boudreau, F., Chappell, W., Ouyang, Z.: Non-destructive ion trap mass analysis at high pressure. Anal. Chem. **83**(3), 685–689 (2011)